energies

MDPI

*Article*

# Study of the Characterisation Method of Effective Two-Phase Seepage Flow in the Construction of Gas Storage Reservoirs

**Guoying Jiao [1], Shijie Zhu [1,*], Fei Xie [2], Shuhe Yang [2], Zuping Xiang [1] and Jiangen Xu [1]**

[1] School of Petroleum and Natural Gas Engineering, Chongqing University of Science & Technology, Chongqing 401331, China
[2] Research Institute of Exploration and Development, Dagang Oilfield Company, PetroChina, Tianjing 300450, China
* Correspondence: zhusj@cqust.edu.cn

**Abstract:** During the rebuilding of a gas reservoir, repeated "strong injection and mining" processes change the seepage capacities of gas and water. Hence, accurately determining the seepage laws of gas and water in a gas storage reservoir is crucial. In this study, a standard relative permeability test was conducted with a one-dimensional core. Additionally, a gas reservoir injection and mining simulation experiment was conducted with a two-dimensional plate. The results show that the relative permeability curve obtained by the one-dimensional core test did not accurately reflect the operation characteristics of the gas storage and the change in the seepage law during the gas reservoir construction. Furthermore, in the two-dimensional plate experiment, the operation mode was restored using the plane radial flow formula, the mutual relationship between the gas and water's effective permeability under different injection stages was established, and the multi-cycle injection operation was accurately described. This method lays the foundation for the construction of gas reservoirs and the establishment of the multi-phase seepage law for gas reservoirs.

**Keywords:** gas storage; injection production simulation; effective permeability; seepage law; two-dimensional simulation experiment



**Citation:** Jiao, G.; Zhu, S.; Xie, F.; Yang, S.; Xiang, Z.; Xu, J. Study of the Characterisation Method of Effective Two-Phase Seepage Flow in the Construction of Gas Storage Reservoirs. *Energies* **2023**, *16*, 242. https://doi.org/10.3390/en16010242

Academic Editor: Hossein Hamidi

Received: 10 November 2022
Revised: 14 December 2022
Accepted: 19 December 2022
Published: 26 December 2022



## 1. Introduction

The purpose of gas storage is to solve the inherent contradictions between natural gas supply and consumption [1], that is, the inherent contradictions between reliable, safe, stable, and continuous gas supply and consumption demand imbalance [2]. With the increasing proportion of natural gas in the energy structure [3], countries around the world are developing more gas storage reservoirs to increase gas storage [4], thereby ensuring peak emergency regulation [5]. To meet the construction needs of gas storage reservoirs [6], depleted gas reservoirs are gradually reconstructed. Meanwhile, the "strong injection and mining" operation in the construction process of gas storage reservoirs significantly affects the throat structure [7] and seepage capacity of the reservoir [8], as well as the size of the gas storage library building space [9] and the long-term operation safety [10]. Therefore, it is particularly important to accurately determine the relative permeability curve rules in the strong injection and mining construction process of gas storage reservoirs [11].

The conventional method for studying the law of fluid seepage is based on relative permeability tests [12]. Hence, to simulate the operation of gas storage reservoirs, experiments were conducted to establish the relationship between the injection–production process and the reverse displacement to determine the relative permeability curves of gas/water, oil/water, and gas/oil. Meanwhile, the injection–production operation of gas storage reservoirs was achieved through repeated displacements. Considering the relative permeability test of oil/water as an example, the specific experimental steps were as follows [13]: (1) The water was first saturated, and then the oil was saturated (oil displaced the water to the bound state). (2) The oil phase permeability in the bound water state was

determined. (3) Water drive oil experiments were performed according to the displacement conditions, and a suitable displacement speed or displacement pressure difference is selected. (4) The direction of the rock sample switched from left to right and they were loaded into the pressure-tapped core based on the displacement conditions. An appropriate displacement speed or pressure difference was selected for the oil/water displacement experiment. (5) The rock sample changed direction from left to right in the pressure-tapped core, and this was repeated to perform multiple relative permeability curve tests for the mutual oil/water drives. In the present study, the underwater phase seepage deviation of the last two rounds of water drive oil binding was within 3% at the end of the oil/water mutual drive experiment. (6) The "J·B·N" method was applied for data processing, and the relative permeability curves were obtained, as shown in Figure 1 [14].

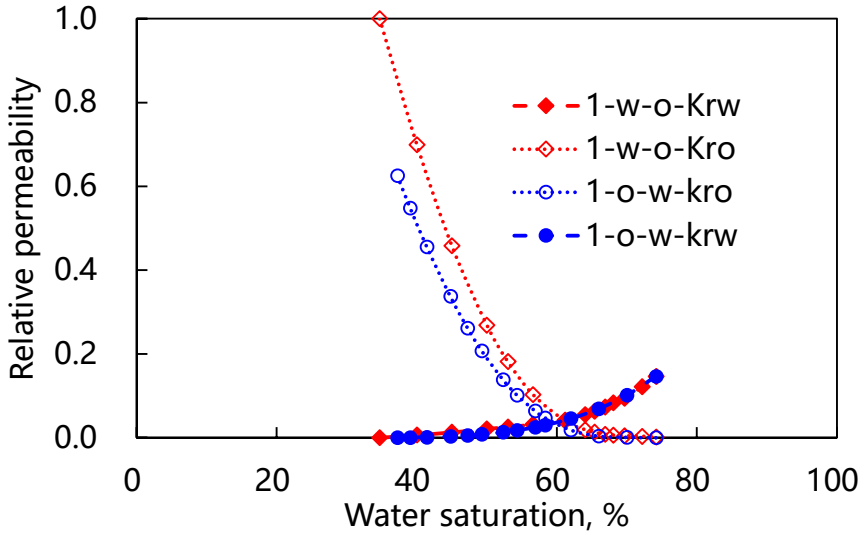


**Figure 1.** Oil/water permeability plot of relative mutual drive.

However, the seepage law in the construction process of gas storage reservoirs cannot be accurately reflected based on the above process because of the following reasons: (1) There are differences in the injection mining and mutual drive methods. The displacement process in the relative permeability test caused steady seepage at a constant speed or pressure. However, the injection and mining process caused unstable seepage at a constant pressure. (2) The relative permeability test simulated the whole process of the reservoir construction (as shown in Figure 1), ranging from bound water saturation to residual oil saturation and vice versa. However, one gas storage injection and mining operation cycle is a very small stage of the gas storage operation. (3) The core ripple efficiency in the relative permeability test was 100%, whereas the injection efficiency in the actual injection process was considerably less than 100%, indicating a large difference in the seepage law. Therefore, to study the seepage law of the gas reservoir, it was necessary to learn from the high-accurate simulation of the appropriate equipment model, adopt a more appropriate method, and establish a more accurate seepage law to lay the foundation for the numerical simulation of the gas reservoir [15].

The scheme optimisation during the construction of an existing gas storage reservoir depends on the reservoir numerical simulation technology, and the core technology is a full-cycle simulation of the injection and production process using the relative permeability data. The accuracy of the relative permeability curve will directly affect the understanding of the simulation results, so it is particularly important to obtain a highly matched relative permeability curve of the gas storage reservoir. Moreover, there is no relevant literature reporting on a new method for measuring the relative permeability curve during the construction of a gas storage reservoir. Thus, considering the influence of sweep efficiency in the injection–production process, this study was conducted using a two-dimensional

plane model. First, the change in the seepage law after multiple rounds of the injection–production process (mutual drive) was determined. Second, combined with the plane radial flow theory, the change in the effective permeability of the gas storage reservoir during the injection–production process was studied. Through the relative permeability curve, which is the essential attribute of the relationship between water saturation and permeability, a highly simulated experiment was designed to analyse the characteristics of the relationship between water saturation and permeability, and a method for analysing the two-phase seepage ability of gas storage reservoirs during the injection–production process was established using a two-dimensional experimental model.

## 2. Experimental Methods

The experiments in this study were divided into a one-dimensional core experiment and a two-dimensional core experiment. The one-dimensional core test was conducted according to the industry standard of a relative permeability curve. A multi-cycle injection and production process of gas storage was simulated using multi-cycle mutual drive [16]. This is the main method for obtaining the multi-cycle injection production relative permeability at this stage. The two-dimensional core experiment was a complete experimental process formed by reducing the injection and mining process of the ore field using the real plane model. Through the description and comparison of the two experimental processes, and combined with the presentation of data, this study provides support for the establishment of new methods.

### *2.1. Experimental Conditions*

Based on the properties of a gas reservoir, a one-dimensional artificial core and a two-dimensional plate were adopted in this study. The specific parameters were as follows:

(1) Experimental water: The viscosity of the formation water was 0.894 mPa·s;

(2) Natural gas: Methane gas was used in the experiment, with a viscosity of 0.0178 mPa·s. Its components are listed in Table 1.

**Table 1.** Methane gas fractions.

| Component | $C_1$ | $C_2$ | $C_3$ | $C_4$ | $C_5$ | $N_2$ | $CO_2$ | He | $H_2$ |
|---|---|---|---|---|---|---|---|---|---|
| Content | 91.41 | 4.93 | 0.96 | 0.41 | 0.24 | 1.63 | 0.06 | 0.29 | 0.07 |

(3) Experimental core: An artificial core comprising quartz sand, solid epoxy resin with an average permeability of 1000 mD, and a flat plate model with a size of 500 × 500 × 20 mm was adopted;

(4) Experimental temperature: The simulated reservoir temperature was 82 °C;

(5) Experimental device: The device comprised a one-dimensional artificial core with a permeability of approximately 800 mD and a two-dimensional plate model, as shown in Figure 2. The inner diameter of the device was 500 × 500 × 20 mm, and the upper limit pressure was 20 MPa.

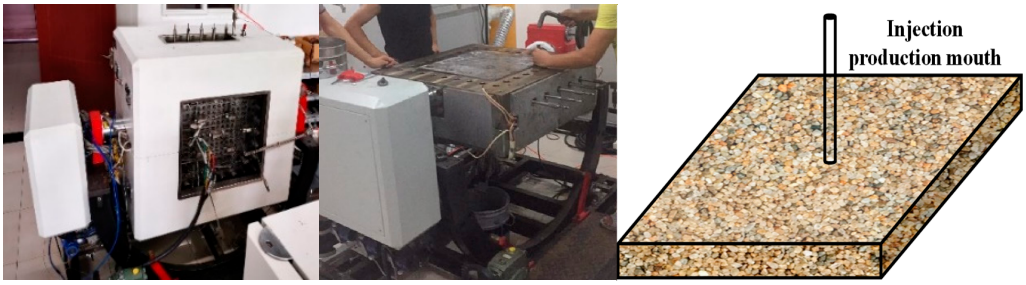


**Figure 2.** Two-dimensional core simulation setup: (**left**) overall appearance; (**middle**) plate placement, (**right**) schematic diagram of the injection and mining method.

### *2.2. Experimental Procedure*

#### 2.2.1. Experimental Procedure of the One-Dimensional Core

The relative permeability test was performed according to industry standards, and the steps are given as follows [17]: (1) The core was dried, and the gas measurements were taken by injecting gas into the core. The permeability of the core was then determined as the absolute permeability. (2) The pore volume/porosity of the core was determined by saturating the rock sample with formation water. (3) The water logging permeability (or absolute permeability) of the rock sample was measured after injecting the formation water into the sample at a constant speed. (4) The gas flooding required that the initial differential pressure could overcome the end effect without turbulence. (5) The displacement pressure difference, cumulative fluid production, cumulative water production, and initial gas breakthrough point were recorded at each displacement time. When the gas drive water reached the residual water state, the gas permeability was measured, and the experiment was terminated.

Based on the one-dimensional two-phase seepage theory and gas state equation, the gas flooding experiment of the rock samples was conducted using the unsteady constant pressure method [18]. The gas production, water production, and differential pressure at both ends of the rock sample at each time point at the outlet of the rock sample during the gas flooding were recorded. Moreover, the J·B·N method (Equations (1)–(8)) was used to calculate the gas/water relative permeability and the corresponding water saturation of the rock samples. Afterwards, the gas/water relative permeability curve was obtained [19].

$$S_{gav} = \frac{V_w}{V_p} \tag{1}$$

$$\frac{K_{rg}}{K_{rw}} = \frac{f_g}{f_w} \times \frac{\mu_g}{\mu_w} \tag{2}$$

$$q_{gi} = \frac{\Delta V_{gi}}{\Delta t} \tag{3}$$

$$f_g = \frac{\Delta V_{gi}}{\Delta V_i} \tag{4}$$

$$K_{rg} = \frac{q_{g\mathrm{i}}}{q_g} \tag{5}$$

$$C = \frac{p_1}{p_2 + \Delta \mathrm{p}} \tag{6}$$

$$q_g = \frac{KA}{\mu_g L} \times \Delta p \tag{7}$$

$$f_w = \frac{\Delta V_{wi}}{\Delta V_i} \tag{8}$$

where $S_{gav}$ is the average gas saturation (%), $V_w$ is the cumulative outlet water volume (mL); $V_p$ is the cumulative export gas volume (mL); $K_{rg}$ is the relative permeability of the gas phase (in decimals); $K_{rw}$ is the relative permeability of the water phase (in decimals); $f_g$ is the gas cut (in decimals); $f_w$ is the water cut (in decimals); $\mu_g$ is the injection gas viscosity (mPa·s); $\mu_w$ is the viscosity of the simulated formation water in the saturated rock samples (mPa·s); $q_{gi}$ is the gas flow rate during the two-phase flow (mL/s); $V_{gi}$ is the gas increment measured at the outlet pressure (mL); $V_i$ is the amount of fluid change at a certain time interval (mL); $q_g$ is the gas flow during the single-phase flow (mL/s); $C$ is the antihypertensive volume factor (in decimals); $p_1$ is the absolute inlet pressure of the rock sample (MPa); $p_2$ is the absolute outlet pressure of the rock sample (MPa); and $V_{wi}$ is the measured water increment at a certain time interval (mL).

2.2.2. Experimental Procedure of the Two-Dimensional Model

(1) The two-dimensional plate model was filled with quartz sand and then properly sealed. The "one note, four minings" mode of saturated formation water and the "four injections, one mining" mode of saturated crude oil were used. The formation water and crude oil were injected at a constant speed (1 mL/min), and the pressure was maintained at 10 MPa;

(2) A multi-cycle injection test was conducted using the following steps: (i) The injection and mining pressure of the actual simulation experiment was 10–17 MPa. (ii) One mining well network was formed at the centre of the model. (iii) In the injection–production experiment, within the upper- and lower-limit operating pressure ranges of the simulated gas storage, the injected gas was gradually pressurised to the target constant pressure, and the injection time (simulated mine injection time) was recorded. Afterwards, a boiling operation was simulated for 1/10 of the injection time, and the exhaust valve was opened. Meanwhile, the time (half of the injection time) was controlled until the pressure at the outlet reached the atmospheric pressure and no water was produced. Step (iii) was then repeated five times, and the output volume was recorded and measured using a gas flow meter. (iv) The injection formed the central well, and the model was injected in the middle and extracted in the middle. Figure 2 shows the experimental setup.

## 3. Results and Discussion

The injection production operation mode in the process of gas storage reservoir construction determines the multi-cycle mutual displacement of gas and water. Therefore, the multi-cycle mutual drive mode was introduced for characterisation based on the relative permeability. In addition, a two-dimensional large plane model was built to conduct multi-cycle injection and production research in combination with actual injection and production parameters, and the operation process of database construction was highly restored. A comparative study of the two methods was expected to establish a highly consistent pattern of the law of infiltration.

### *3.1. Two-Phase Percolation Experiment of the One-Dimensional Core*

The relative permeability curves of the gas/water mixture were obtained, as shown in Figure 3.

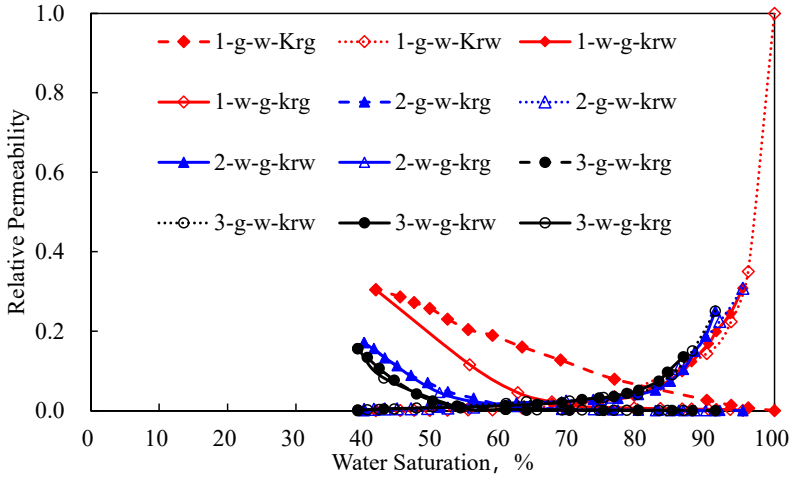


**Figure 3.** Relative permeability curves of gas/water in the highly permeable core.

Based on the relative permeability curve under the target core condition, the following conclusions can be drawn: (1) The seepage capacities of the gas drive water and water drive gas were based on two laws, which were caused by the wetting characteristics of the core; hence, the simulation resulted in an inaccurate with the standard relative permeability curve compared to the experimental means. (2) After multiple gas/water mutual drives, the

residual gas saturation and bound water saturation changed, indicating that the effective storage capacity after multiple rounds was reduced and not conducive to an increase in the gas storage space. The large decrease in the seepage capacity indicates a decrease in gas storage at the later stage of secondary injection mining; however, this is obviously different from the actual situation characteristics of the gas reservoir, which showed that the seepage curve of the one-dimensional core and gas storage simulation was limited.

### *3.2. Two-Phase Seepage Experiment of the Two-Dimensional Plate*

#### 3.2.1. Experimental Result

(1) The gas injection time, the shut-in time, the oil return time during the simulation process, and the experimental data of the water and gas productions are listed in Table 2, and the single-cycle and cumulative extraction degrees are shown in Figure 4.

**Table 2.** Gas and water production under different injection and mining cycles.

| Construction/Water Characteristics | Injection–Production Cycle | | | | | | | | Remarks |
|---|---|---|---|---|---|---|---|---|---|
| | One | Two | Three | Four | Five | Six | Seven | Eight | |
| Gas injection time (min) | 25 | 23 | 20 | 19 | 15 | 15 | 15 | 10 | The saturated water volume was 2010 mL |
| Well shut-in time (min) | 2.5 | 2.5 | 2 | 2 | 1.5 | 1.5 | 1.5 | 1 | |
| Oil return time (min) | 10 | 11 | 10 | 10 | 7 | 7 | 7 | 5 | |
| Water production (mL) | 302 | 206 | 131 | 97 | 88 | 65 | 41 | 23 | 953 |
| Gas production (L) | 7.2 | 19.4 | 25.9 | 36.4 | 46.1 | 51.8 | 57.5 | 64.8 | 309.1 |

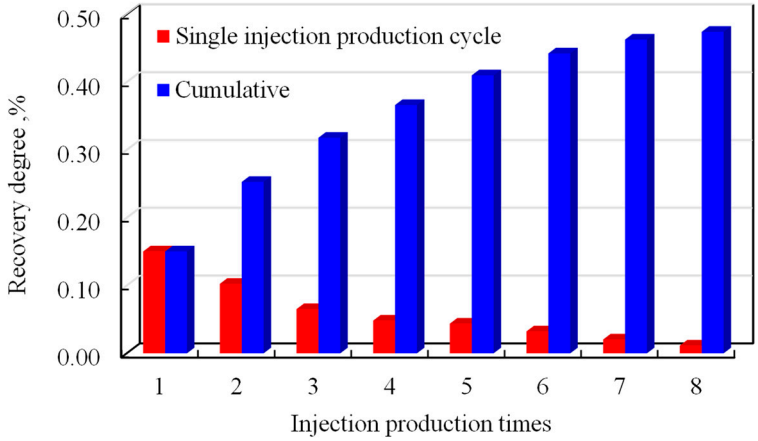


**Figure 4.** Extraction degrees under different injection cycles.

As shown in Figure 4 and Table 2, during the injection and mining operations of the gas storage tank, the water could be collected by extracting the reservoir fluid to excavate more gas storage space. With the progress of the injection and mining cycles, the water extraction degree in a single cycle gradually decreased, whereas the cumulative extraction degree gradually increased and stabilised until no more water was produced, thereby achieving the bound water conditions, that is, the maximum effective storage space was reached. The analysis indicates that after the multi-cycle injection and extraction, the remaining fluid of the reservoir decreased, and the aqueous seepage capacity was significantly reduced; thus, the extraction degree gradually decreased. The large increase in gas output was because of the large increase in the gas storage space, causing more gas to be injected under the upper-limit pressure of the gas injection.

It can be deduced from Figure 4 that the water saturation decreased with the injection cycle, and the production velocity per unit of time indicates that the permeability of the effective gas injection space in the model and the gas output (gas saturation) increased.

This law is similar to the two-phase seepage law expressed in the gas/water relative permeability curve, indicating that the multi-cycle injection and mining process can also be used to build a similar relative permeability curve, which is the seepage law most consistent with the injection and mining process.

3.2.2. Method Principle

Considering the two-dimensional plate model, the plane radial flow formula was adopted to calculate the seepage flow capacity, which is important for predicting and determining the flow capacity of a gas well.

One of the most important scenarios for applying the planar radial flow formula is the determination of the effective permeability of the reservoir. Based on the relevant literature [20,21], the planar radial flow formula is given by:

$$\frac{P_e - P_{wf}}{m_t} = \frac{\lambda^n}{2\pi Kh} m_t + \frac{1}{2\pi Kh}\left(\ln \frac{r_e}{r_w} + S\right) \quad (9)$$

where $P_e$ is the reservoir supply pressure (MPa); $P_{wf}$ is the flow pressure at the well bottom (MPa); $m_t$ is the mass flow (kg/d); $\lambda$ is the turbulent effect coefficient ($\lambda \geq 1$; $\lambda = 1$ is the laminar flow); n is the representation index of high and low speeds; $K$ is the effective permeability of the reservoir (mD); $h$ is the effective thickness of the reservoir (m); $r_e$ is the water supply radius (m); $r_w$ is the Holbore radius (m); and $S$ is the epidermal coefficient.

In Equation (9), the size of the model was determined to be 500 × 500 × 20 mm, the injection well was in the centre of the model, and the experimental research pipeline was a 2 mm capillary. Additionally, the oil discharge radius, wellbore radius, and reservoir thickness were determined to be 250, 1, and 20 mm, respectively. Furthermore, both the formation water and natural gas were determined based on the basic experimental parameters, and the mass flow was determined from the results of the two-dimensional plane radial flow. Subsequently, the Reynolds equation was applied to determine the laminar flow below 3 MPa and the turbulence above 3 MPa, depending on the flow velocity changes resulting from different pressures. The application of the n was then determined, and the turbulence coefficient was obtained using empirical values.

3.2.3. Method Application Examples

The steps for determining the changes in the effective permeability during the gas storage injection were as follows: (1) Based on the physical conditions of the target block, a two-dimensional large-scale plane rock plate model was constructed, and the relevant parameters (oil/water physical properties, pressure, temperature, and so on) were determined. (2) Multiple rounds of gas injection and production tests were performed according to the injection and production operation scheme of the gas storage in the target reservoir. (3) The plane radial flow formula (Equation (9)) was used to calculate the effective permeability based on the changes in water/gas production. (4) The water saturation was calculated according to the recovery degree, and the relative permeability curve was constructed in combination with the calculated effective permeability.

(2) Equation (9) was used to calculate the mean core permeability at the current cycle from the actual experimental model in 2D (see Table 3).

**Table 3.** Permeability values for the calculation of the two-dimensional model.

| Period | 1 | 2 | 3 | 4 | 5 | 6 | 7 | 8 |
|---|---|---|---|---|---|---|---|---|
| Mean water-phase permeability (mD) | 990 | 870 | 740 | 540 | 490 | 360 | 230 | 130 |
| Mean gas-phase permeability (mD) | 120 | 240 | 320 | 450 | 570 | 640 | 710 | 800 |

As presented in Table 3, the permeability values reflect the average permeability characteristics of the core after an injection and mining cycle, which are the equilibrium

values after its strong injection and mining. This reflects the impact of the injection and mining process in which the water content saturation and the water-phase permeability capacity gradually decreased, whereas the gas-phase permeability capacity gradually increased. The experimental data present the key parameters of the permeability curve. Therefore, the saturation and fluid volume data under each cycle were applied to build a relationship between the permeability and saturation, and the data were combined with the absolute permeability measured by the core to calculate the relative permeability and the change in the relative permeability (see Figure 5).

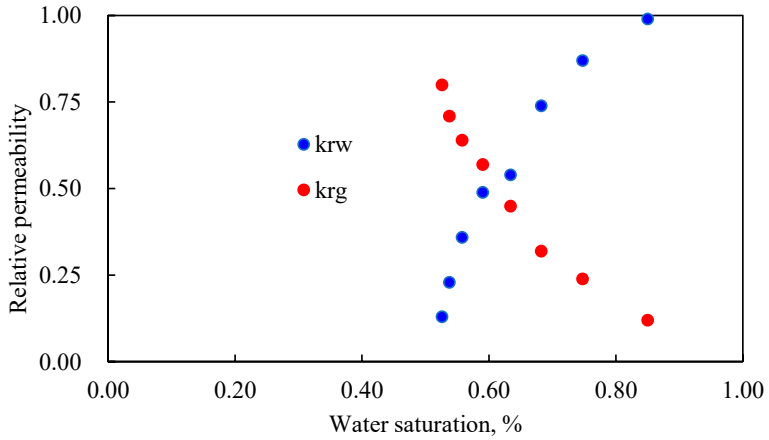


**Figure 5.** Relative permeability plot.

The relative permeability curve features shown in Figure 5 are almost consistent with those of the one-dimensional core test; however, the significance of the seepage law is different. The relative permeability curve was a relatively stable seepage capacity value after the mutual injection and mining process. This reflects the influence of the injection and mining process on the seepage law of gas storage through continuous multi-cycle gas injections.

### *3.3. Flow Difference between the One-Dimensional Core and Two-Dimensional Plate*

Figures 3 and 5 show the relative permeability curves under the two experimental conditions. In fact, the relative permeability curves themselves are the simulated features of a reservoir and gas reservoir from the original state to extreme development, or the simulated process of oil and gas reservoir formation. Although the simulation of the injection–production process was repeated several times, the results do not accurately describe the injection and production of gas storage. Therefore, the set of curves adopted in the multiple rounds of the mutual drive process is not accurate.

The seepage curve constructed by the injection simulation experiment of the two-dimensional rock plate represents the final seepage law of the gas reservoir under each injection and mining cycle and the entire construction process of the simulated gas storage reservoir. Based on the data of the one-dimensional permeability experiment, the relative permeability corresponding to the water content saturation after the two-dimensional injection and mining experiment is given by Equation (1). The calculation results were compared with the actual data, as presented in Table 4.

**Table 4.** Multi-cycle injection and production results calculated from the relative permeability curve of the one-dimensional core.

| Period | 1 | 2 | 3 | 4 | 5 | 6 | 7 | 8 |
|---|---|---|---|---|---|---|---|---|
| Water yield calculated for the first secondary phase seepage (mL) | 217 | 153 | 112 | 87 | 74 | 54 | 32 | 5 |
| Water yield calculated for the third round of the secondary phase seepage (mL) | 117 | 81 | 63 | 43 | 18 | 14 | 9 | 2 |
| Actual fluid yield (mL) | 302 | 206 | 131 | 97 | 88 | 65 | 41 | 23 |

The relative permeability curve obtained from the corresponding water saturation in the injection and mining core was significantly lower than that of the actual experimental data. Based on the analysis, the two-dimensional core model simulated the injection process of gas storage, and the strong injection and mining production mode significantly enhanced the seepage capacity of the fluid in porous media and relatively increased its effective permeability. Meanwhile, the water-phase permeability capacity after the third mutual drive in the phase–seepage curve significantly decreased, with a more significant decrease in the water-production capacity. Therefore, the relative permeability curve obtained by the one-dimensional core does not accurately reflect the seepage law of the gas storage injection operation, whereas the two-dimensional plate experiment more accurately reflects the seepage law of the gas storage injection operation time.

The relative permeability curve obtained by the two-dimensional experimental model was analysed and fitted during the process of the reservoir numerical simulation. The results are closer to the field data than the one-dimensional relative permeability experimental curve. This lays a foundation for accurately guiding the development of field tests.

## 4. Conclusions

(1) During multiple gas/water mutual drive rounds, the seepage capacity of the core flow significantly decreased. Thus, the permeability capacity of a multi-cycle injection operation could not be scaled with a single relative permeability curve.

(2) The two-dimensional simulation experiment accurately simulated the operation process of gas storage, and gas injection improved the storage capacity. With each injection cycle, the synergistic water extraction capacity gradually decreased. Moreover, the relative permeability curve obtained by the two-dimensional simulation model experiment and the plane radial flow formula was the seepage law after the multi-cycle injection and mining process. Hence, the phase–seepage relationship derived from the two-dimensional simulation experiment is more consistent with the results of the gas storage injection operation.

**Author Contributions:** Methodology, S.Z.; Software, S.Y.; Formal analysis, G.J.; Resources, F.X.; Writing—original draft, G.J. and S.Z.; Writing—review & editing, Z.X.; Funding acquisition, S.Z. and J.X. All authors have read and agreed to the published version of the manuscript.

**Funding:** This work was funded by the Natural Science Foundation of Chongqing (cstc2021jcyj-msxmX0522 and cstc2020jcyj-msxmX0163), the Science and Technology Research Program of Chongqing Municipal Education Commission (KJQN202001518), and the Scientific Research Funding Project of Chongqing University of Science and Technology (ckrc2021004).

**Data Availability Statement:** The data supporting the findings of this study are available from the corresponding author upon reasonable request.

**Conflicts of Interest:** The authors declare no conflict of interest.

## References


1. Zheng, D.; Xu, H.; Wang, J.; Sun, J.; Zhao, K.; Li, C.; Shi, L.; Tang, L. Key evaluation techniques in the process of gas reservoir being converted into underground gas storage. *Pet. Explor. Dev.* **2017**, *44*, 794–801. [CrossRef]
2. Zeng, D.; Zhang, J.; Zhang, G.; Mi, L. Research progress of Sinopec's key underground gas storage construction technologies. *Nat. Gas Ind.* **2020**, *40*, 115–123.
3. Ma, X.; Ding, G. *China Underground Natural Gas Storage*; Petroleum Industry Press: Beijing, China, 2018.
4. Tuna, E.; Can, P. Natural gas underground storage and oil recovery with horizontal wells. *J. Pet. Sci. Eng.* **2020**, *187*, 106753.
5. Liu, W.; Jiang, D.; Chen, J.; Daemen, J.J.K.; Tang, K.; Wu, F. Comprehensive feasibility study of two-well-horizontal caverns for natural gas storage in thinly-bedded salt rocks in China. *Energy* **2017**, *143*, 1006–1019. [CrossRef]
6. Zeng, S. *Study on Seepage Mechanism and Application of Gas Storage Reconstruction in Late High Water Cut Reservoir*; Southwest Petroleum Institute: Chengdu, China, 2005.
7. He, S.; Men, C.; Zhou, J.; Wu, Z. Study on injection production seepage characteristics of Da zhang tuo gas reservoir. *Nat. Gas Ind.* **2006**, *5*, 90–92.
8. Ban, F.; Gao, S.; Wang, J. Gas Injection-production Mechanism of Gas Storage in Depleted Oil Reservoirs. *Nat. Gas Geosci.* **2009**, *20*, 1005–1008.
9. Wang, J.; Guo, P.; Jiang, F. The Physical Simulation Study on the Gas-Drive Multiphase flow Mechanism of Aquifer Gas Storage. *Nat. Gas Geosci.* **2006**, *4*, 597–600.
10. Lei, S.; Guangzhi, L.; Wei, X.; Shusheng, G.; Tong, G. Gas-water percolation mechanism in an underground storage built on a water-drive sandstone gas reservoir. *Nat. Gas Ind.* **2012**, *32*, 85–87.
11. He, X.; Huang, S.; Sun, C.; Xu, J.; Zhang, X.; Yang, X. Gas-water relative permeability variation in multi-cycle injection production of underground gas storage in flooded depleted gas reservoir. *Oil Gas Storage Transp.* **2015**, *34*, 150–153.
12. Shi, L.; Wang, J.; Zhu, H.; Duan, Y. Microscopic percolation laws of gas and water in underground gas storages rebuilt from water-invasion gas reservoirs. *Nat. Gas Explor. Dev.* **2020**, *43*, 58–63.
13. Ding, Y.; Zhang, Q.; Shi, L.; Sun, j.; Jiang, S. Characteristics of Underground Gas Storage Built on Carbonate Gas Reservoir in S Region, North China. *Sci. Technol. Guide* **2014**, *32*, 51–54.
14. Sun, C.; Hou, J.; Shi, L.; Liang, C.; Gan, Z. A physical simulation experimental system for injection-withdrawal operation of gas reservoir underground gas storage and its application. *Nat. Gas Ind.* **2016**, *36*, 58–61.
15. Niu, C. *Seepage Displacement and Operating Simulation of Fractured Underground Natural Gas Storage Reservoir*; Harbin Institute of technology: Harbin, China, 2016.
16. Zhu, S. *Study on the Timing of Polymer Flooding in Common Heavy Oil Reservoir*; Southwest Petroleum University: Chengdu, China, 2015.
17. Sinan, Z.H.U.; Junchang, S.U.N.; Guoqi, W.E.I.; Zheng, D.; Jieming, W.A.N.G.; Lei, S.H.I.; Xianshan, L.I.U. Numerical simulation-based correction of relative permeability hysteresis in water-invaded underground gas storage during multi-cycle injection and production. *Pet. Explor. Dev.* **2021**, *48*, 190–200.
18. Li, C.; Li, X.; Gao, S.; Liu, H.; You, S.; Fang, F.; Shen, W. Experiment on gas-water two-phase seepage and inflow performance curves of gas wells in carbonate reservoirs: A case study of Long wang miao Formation and Deng ying Formation in Gaoshiti-Moxi block, Sichuan Basin, SW China. *Pet. Explor. Dev.* **2017**, *44*, 930–938. [CrossRef]
19. Zhu, S.; Shi, L.; Zhang, J.; Li, T.; Wang, G.; Xue, X.; Ye, Z. Application method of relative permeability curve to judge the timing of polymer flooding to polymer injection. *Reserv. Eval. Dev.* **2020**, *10*, 128–134.
20. Zhai, Y. *Seepage Mechanics*; Petroleum Industry Press: Beijing, China, 2016.
21. Yao, J.; Gu, J.; Lu, A. *Principles and Methods of Reservoir Engineering*; China University of Petroleum Press: Dongying, China, 2016.